EMC behavior of PWM inverter structure based on coupled interleaved cells using Intercell Transformers

Cyrille Gautier, Fabien Adam, Eric Labouré, Bertrand Revol

EMC Behavior of PWM Inverter structure based on Coupled Interleaved Cells using Intercell Transformers

Cyrille Gautier[1], Fabien Adam[1], Eric Labouré[2], Bertrand Revol[1]
SATIE, ENS Cachan, CNRS, UniverSud ([1])
61 av. du President Wilson
94 230 Cachan, France
Tel: +33 1 47 40 21 08
LGEP, CNRS, UniverSud ([2])
11, rue Joliot Curie, Plateau de Moulon,
91192 Gif sur Yvette, France
cyrille.gautier@satie.ens-cachan.fr

Abstract

In this paper, the innovative structure of a PWM Multicell Interleaved Converter using Intercell Transformers is presented, and an accurate EMC oriented model is proposed. In such topologies, regarding spectral contents of common-mode voltage, the fundamental frequency and the harmonics are shifted by a factor q with respect to the switching frequency, where q is the number of interleaved cells. The EMI and especially the common mode behavior of this family of power converters are therefore discussed. A prototype has been designed, allowing comparison between measurement and simulations. Thus, the modeling approach is validated, and the positive effects on common-mode conducted interferences are confirmed.

Keywords

EMC, Power Converter, PWM Interleaved Inverters, Intercell Transformers, common mode interferences

Introduction

The diversification of power converters structures can provide more power efficient solutions, adapted to operating conditions. In order to achieve greater power density and because of EMC filter volume, EMC became one of the main design criterion. In this paper, we will focus on natural filtering behavior of a PWM Multicell Interleaved Inverter using Intercell Transformers, and on the modeling process based on EMC requirements. This inverter is intended for three-phase variable-speed drives systems, but, in order to simplify, only one multicell phase of the Inverter is studied in this paper. The main goal of the modeling process is to obtain realistic waveforms of conducted interferences from functional model, in order to compare EMC performances of different converter structures. Another goal of these models is to allow test of different control strategies to optimize spectrum repartition of conducted emissions. A prototype has been specifically designed in order to allow testing of different interleaved converter structures, and comparison between measurement and simulation results. Eventually, the positive effects of the natural filtering behavior of the presented converter on common-mode conducted interferences and over-voltage occurring at power cable load side are presented.

I. Inverter structure

I.1 Multicell Interleaved Converters with intercell transformers

Multicell Interleaved Converters with intercell transformers (ICT) have proved to be suitable for high current and fast transient response [1], and also permit a real improvement on the magnetic part of the output filters [2]. This structure is now studied regarding EMC behavior. Each phase of the inverter consists of q elementary half bridge inverters connected in parallel, switching at the same frequency f, in order to create an interleaved voltage system applied to the ICT. The ICT is realized with separate transformers and a cyclic-cascade topology [3]. The schematic of one phase in the case of a 6 cells structure associated with 6 ICTs, is presented figure 1.

The operating mode of ICTs produces a combination of the q-phase voltages associated with a filtering function, resulting in a q-level quasi-sinusoïdal waveform for the output voltage Vs.

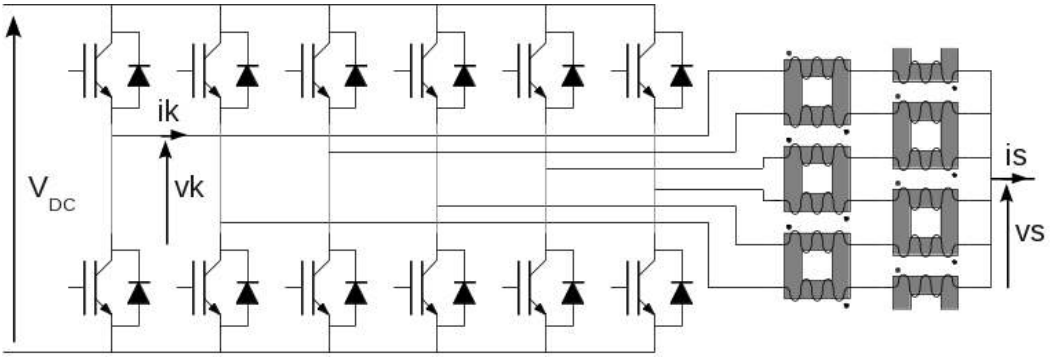

Fig. 1: One phase of the Multicell Interleaved Inverter with intercell transformers (cyclic-cascade).

Two calculated waveforms, in the case of a six phase interleaved inverter, are shown in figure 2 : the left one (Fig. 2.a) corresponds to a 6 level interleaved system without filtering effects, and the right one (Fig. 2.b) with filtering effects, depending on the load impedance.

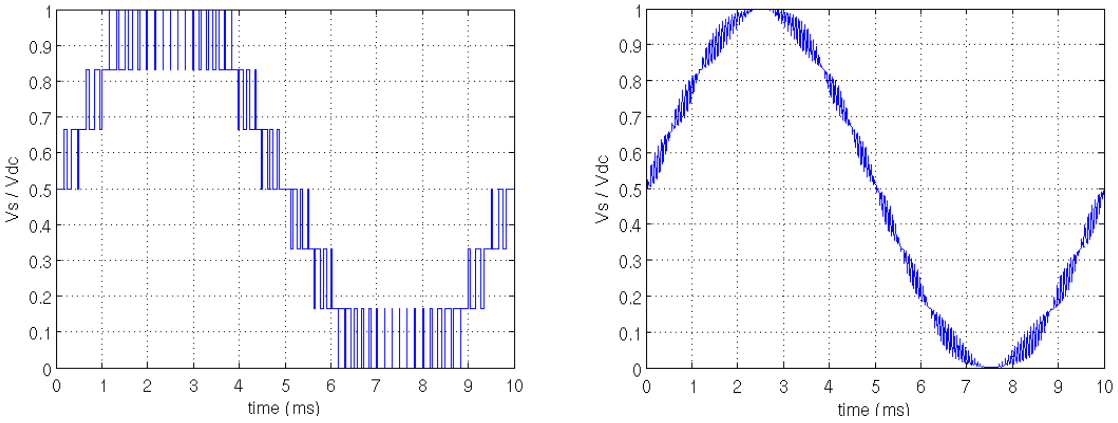

Fig. 2: Output voltage *vs* of a 6 Cells Interleaved Inverter, without (2.a) and with (2.b) filtering effects

The switching frequency has been decreased, and the inductance value has been lowered to show the effects of interleaving and filtering on the output voltage. However, concerning fig 2.b, the filtering effects and therefore the output voltage waveform are very dependent on the load impedance. Anyway, the increase of the apparent switching frequency at the output of the inverter, compared to a one cell inverter structure, and the filtering effects provided by the magnetic coupler, can be very interesting regarding EMC point of view.

I.2 Experimental setup and prototype

The experimental setup is based on a versatile multicell architecture, associated with the needed digital controller. Such versatile power electronics Test-Bench architecture has been presented in [4], allowing test and verification of different converter topologies and control strategies without the renewed requirement of a major hardware effort. Our platform has been designed to enable testing of different configurations of interleaved converters, thus the digital command of the structure is DSP-based and allows an easier implementation of different command schemes. Current and voltage measurement for each phase, as well as output current (i_k) measurement of each cell are implemented. High-speed analog to digital conversion are performed using internal DSP converters. Due to the large number of switching cells, the DSP is associated with a FPGA device which generates the PWM signals, ensuring high accuracy on command timing, and delivering the gating signals to the drivers of each cell. It is important to note that the accuracy provided by the use of high frequency digital devices is needed to achieve current balancing in the switching cells and in the ICTs. In other hand, these new converter architectures are complex, involving numerous switching cells and the associated drivers.

The command schemes to ensure balancing are complex too, leading to a high computing power and a good accuracy on command timings. Eventually, the management of a faulty cell is difficult due to the high coupling between the cells. However, applications that require high integration density or those involving long cable length should be improved using these structures. The prototype, presented on figure 3 is a three phase inverter, each phase consisting of six switching cells and six ICTs according to the structure shown on figure 1. This inverter is connected to the load using a ten meters long cable.

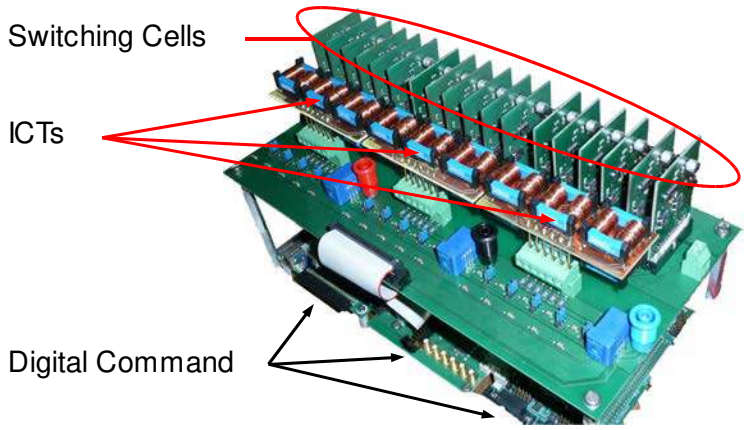

Fig. 3: Three phase inverter, 6 switching cells with 6 ICTs per phase (3x6 structure)

II. Modeling approach

The designers of variable-speed drives systems have to solve a major challenge regarding the EMC constraints. Study of EMC disturbances caused by the association of energy source, power converter, power cable and electric motor, is essential, and have to be considered at the design stage [6]. Our goal is to evaluate EMC behavior of the power converter structure, and to develop a generic approach of the EMC modeling stage. Complex EMC systems are more often modeled using frequency approach, whereas the equipment model, such as a power converter, can be more accurately simulated using component approach and time domain simulation. Some trade-offs have to be found, especially one about the accuracy of the model versus the complexity of parameters extraction and computation effort required to use this model. In the following paragraph of this paper, we will detail the modeling process and present the results we obtained based on the study of one phase of the prototype connected to the load by one of the conductors of the power cable, as shown in figure 4.

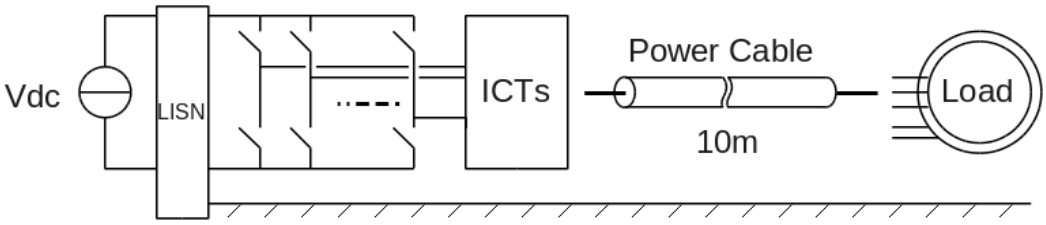

Fig. 4: One phase of a variable speed drive system

II.1 Surge voltage at the load side of the power cable

The propagation of the voltages fronts delivered by power converter along the power cable leads to surge voltages across the load. Our aim is to determine these adverse effects, especially in order to estimate the windings insulation lifetime when the load is an electrical motor. It is well known in power electronic community that switching of semi-conductors components leading to high voltage and current transients, are the main sources of conducted interferences [6]. However, multicell transformers are connected with interleaved switching cells, and this statement must be refined. Thus, the impedance of the interferences sources, as the propagating paths and mode conversion paths must be clearly identified.

Load and cable global model

The surge voltage, due to propagation and mismatching effects is mainly a time domain phenomenon. However, in order to have a fast and efficient computation, a frequency domain approach has been

chosen to model the cable. Such models, based on thin wire approximation and TLM method, have already been established and tested [7]. The conductors and the shielding geometry, as the ground plane if any, are taken into account, modeling skin and proximity effects versus frequency for the components of the model. Propagation effects are also modeled, depending on the cable length L. The impedance behavior of the load is measured using HP4194A impedance analyzer. These results are set together to define the global model of the cable and the load (fig. 5).

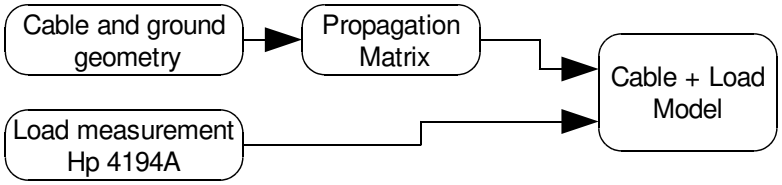

Fig. 5: Global modeling of the power cable and the load

This model is represented by a frequency-dependent matrix that allows to compute the voltages and currents v(L) and i(L) at the load side of the cable according to the voltages and currents v(0) and i(0) applied by the inverter at the converter side, as defined by the equation (1). Experimental data for the load and for a 10m length cable connected to the load have been measured versus frequency. The model of the cable, and the matrix corresponding to the cable and the load, have been calculated.

$$\begin{bmatrix} v(L) \\ i(L) \end{bmatrix} = \begin{bmatrix} \Phi_{11} & \Phi_{12} \\ \Phi_{21} & \Phi_{22} \end{bmatrix} \begin{bmatrix} v(0) \\ i(0) \end{bmatrix} \quad (1)$$

Regarding the common-mode impedance Z_{CM}, the experimental data and the computed one are shown in figure 6. The calculated results for the cable and the load are compared to the measured one with a good agreement. From this model, the impedance driven by the single phase inverter Z_L can be derived.

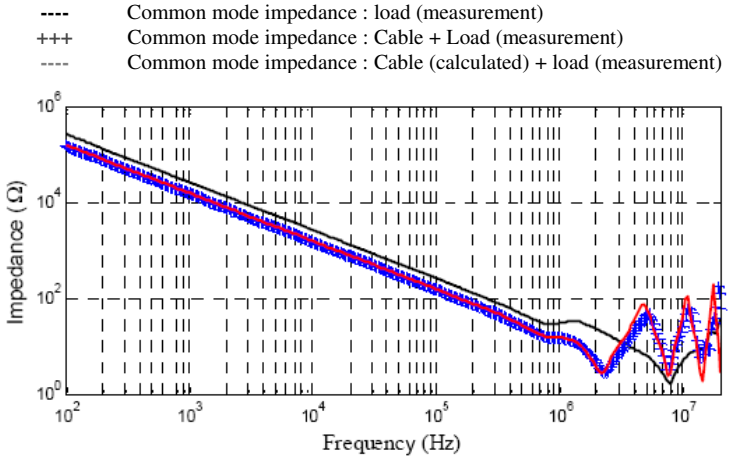

Fig. 6: common-mode impedance of the electrical motor, and for the cable and the motor set together

Model of the source

The transient voltages generated by the switching cells are the main source of transient disturbances, thus, they have to be modeled accurately. Regarding the control strategies, the PWM scheme applied to the q switching cells are $2\pi/q$ phase shifted. Mainly due to the dead time and the gate charge of the IGBT, the driver stage modifies the real switching times, compared to the theoretical one defined by the numerical control signals. However, at first glance, these phenomena can be considered of second order. Therefore we can consider in our model that the 0V and V_{DC} states applied to the coupling cells are regularly time shifted.

As the main source of surge voltages at the far end of the cable, the voltage transients at the output of the switching cells have to be modeled accurately, nevertheless they are heavily dependent on the manufacturing of the power converter. Depending on whether the modeling process is done at design stage or after the completion of an initial prototype, the knowledge we may have on these transients is quite different.

Thus, we will present four different approaches, more and more accurate, of this modeling stage :
The easiest way to represent the switching cells output voltages is to use trapezoidal waveforms, with different rise time and fall time. The difficulty lies in the calculation of the transition times according to power components and circuit topology.
A more sophisticated approach is to decompose the transitions by a piecewise linear approximation, which required experimental data of the transient waveform.
A third method consists on filtering the square theoretical PWM waveforms. The transfer function of the low-pass filter, of first, second or third order, have to be optimized to get the more realistic signals during commutations. The main parameters are directly related to the physics of power components (gate charge) and routing (parasitic inductance). This method was applied to estimate the spectral content of the converter output voltage with good results [5].
Finally, the last way used to reproduce these voltage transients is based on the correlation between PWM patterns and experimental data during rising edge and falling edge. The best results regarding these time dependent effects were obtained using this method and the computed spectral contents of common-mode voltage will be presented in part III.

Intercell transformers

Considering the generic case of a q cells inverter presented figure 1, where $[V_k]_q$ and $[I_k]_q$ are the q voltages and currents at the outputs of the cells as defined by the equation (2) and (3). The magnetic coupling system, composed of the q ICTs, leads to input voltages $[V_k]_q$ summation combined with a filtering effect. This function can be transcribed using matrix equation (4) :

$$[V_k]_q = (v_1, v_2, \ldots, v_q)^T \tag{2}$$

$$[I_k]_q = (i_1, i_2, \ldots, i_q)^T \tag{3}$$

$$\begin{pmatrix} v_1 - v_s \\ \vdots \\ v_q - v_s \end{pmatrix} = (Z) \begin{pmatrix} i_1 \\ \vdots \\ i_q \end{pmatrix} \tag{4}$$

The Z matrix, of dimension q x q, is an intrinsic part of the magnetic coupling system. This matrix is highly dependent upon the realization of the ICTs and its role is predominant in the proposed model. It can be associated with the cable and load impedance Z_L using equation (5), where $[I_d]_q$ is the q x q identity matrix.

$$\begin{pmatrix} v_1 - v_s \\ \vdots \\ v_q - v_s \end{pmatrix} = \left(Z + Z_L . [I_d]_q\right) \begin{pmatrix} i_1 \\ \vdots \\ i_q \end{pmatrix} \tag{5}$$

With the knowledge of the control strategy of the inverter, which imposes the voltage system $[V_k]_q$, the currents flowing through the structure can be calculated by inverting the equation (5). The computation of the $[I_k]_q$ currents is very interesting as they are required to define the characteristics of the magnetic components. They can also be used to calculate the electromagnetic field radiated by the ICTs. More important, the inverter output characteristics could be computed using these currents.
One of the drawback of this method is to required the manufactured magnetic devices to determine the elements of the Z matrix. Moreover, a significant number of measures are to be achieved (q^2 as a maximum) to fulfill the matrix. In the case of a magnetic coupling system made of q identical intercell transformers, we propose to use the symmetry of the system to overcome this problem. It must be possible to use the electrical characteristics measurements of only one ICT to get the knowledge of the whole system characteristics. This idea is also justified because the magnetic coupling system has to be as symmetric as possible from a functional point of view.
Experimental data of the short-circuit impedance Z_{SC}, measured across one winding as the other is shorted, and the open-circuit impedance Z_{OC}, measured across the same winding as the other is open are used to calculate the elements of the Z matrix. The impedance matrix can be built using the following relationship (6).

$$Z_{nm}=\begin{cases} 2Z_{OC} & when\, m=n \\ -\sqrt{Z_{OC}\left(Z_{OC}-Z_{SC}\right)} & when\, m\equiv(n\pm1)\,mod\,q \\ 0 & when\, others \end{cases} \quad (6)$$

The assumptions made to obtain these relations is that the magnetic coupling between intercell transformers are negligible compared to their own parasitic behavior.

II.2 Model validation

The proposed full modeling process is presented figure 7. We decided to compute the common mode current generated by the converter and the voltage at the load side of the cable, because these are two important EMC behavior of the studied system. These disturbances quantities are obtained depending on converter command strategy, in order to compare EMC behavior of new structures of converter with that of a classical two voltage level inverter.

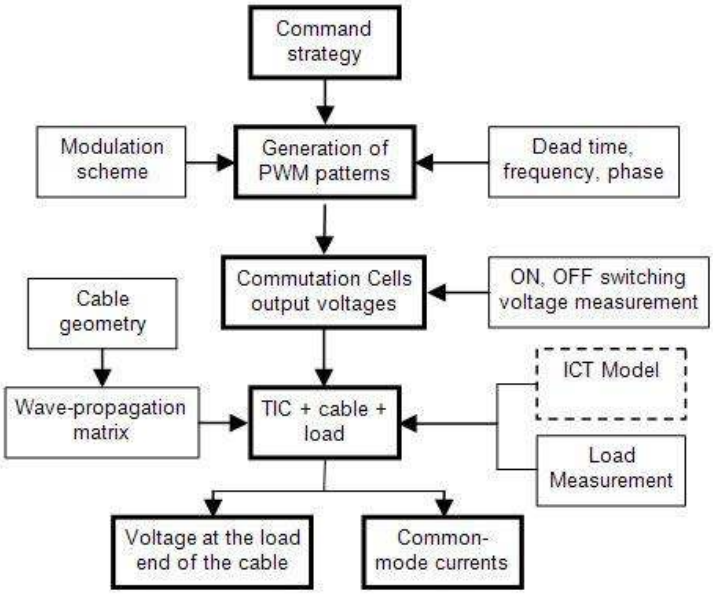

Fig. 7: Modeling process

Results for the simulated (blue) and measured (red) voltage across the load of the multicell inverter are presented in figure 8, compared with that of a two-level inverter (gray).

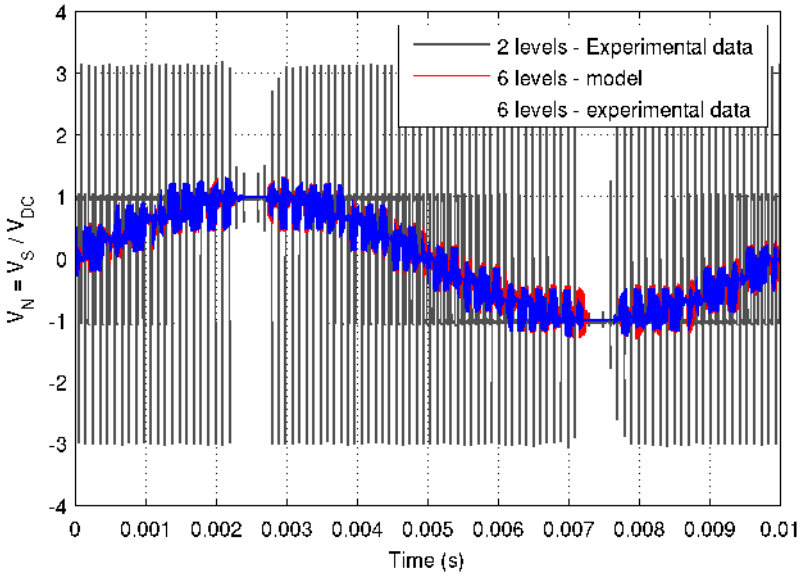

Fig. 8: Voltage across the load at the cable end

A zoom on a switching period is shown in figure 9. The normalized voltage $V_N = V_S / V_{DC}$ has been determined at the end of a ten meter length power cable, for a conventional and a multicell converter supplying the load with the same RMS voltage at the fundamental frequency. The load has been chosen to have an impedance mismatch with the cable, which amplifies voltage surges. It can be noticed that in the case of the two level inverter, the surge voltages reached three times the DC voltage. Such constraints are very strong regarding the insulators of an electrical machine.

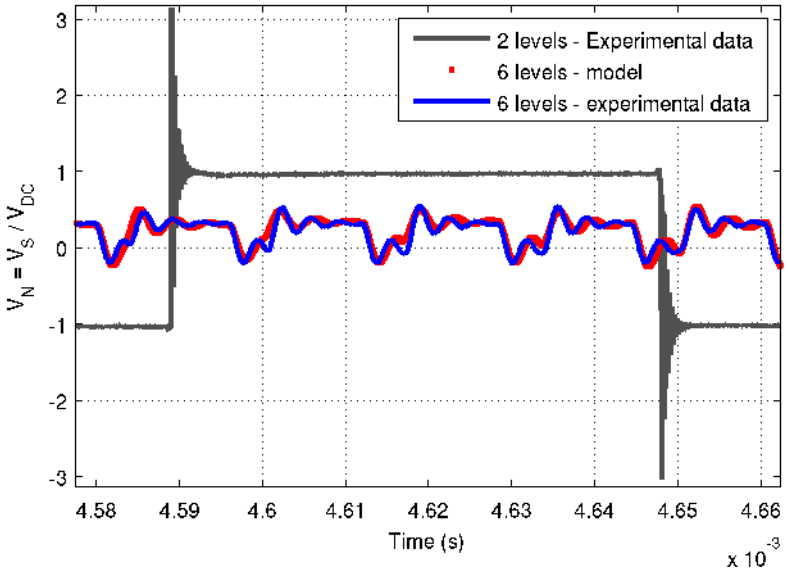

Fig. 9: Zoom on a switching period of the voltage across the load at the cable end

As shown in figure 8, the filtering effect and the decrease of the transient amplitude of the multicell converter are clearly demonstrated, and these constraints are greatly reduced. Furthermore, the good correlation between experimental data and simulation results, as presented in figure 9, leads to validate the modeling process exposed previously.

III. Common-mode currents

Our main goal is to determine the EMC behavior regarding the outputs of the converter as we want to compare the EMC performances of a multicell Interleaved Inverter with ICTs with those of a classical one.

III.1 Spectral content of the output voltage

A model of the intrinsic source of the converter must be established in order to estimate the common mode disturbances. Considering the output of the converter, the common mode voltage of the converter will impose the common mode current which flows through the cable and the load. Assuming that the DC Bus voltage is constant, the common mode voltage is equal to the output voltage. We must compare the spectral contents calculated using the simulation results based on the source model to experimental results. The good agreement of these results, as shown in figure 10, validates the proposed modeling approach.

These results are interesting for several reasons. First, we must notice the absence of spectral signals at the switching frequency, chosen equal to 10kHz. The first spectral signal of major amplitude is at 60kHz, which is q times the switching frequency in the generic case. The corollary of this is that spectral content of the disturbances is reduced. Secondly, the amplitude of harmonics begins to drop at a rate of 40 dB per decade, before rising above 20 MHz. This rapid decrease of the spectrum amplitude is mainly due to the filtering effect of the intercell transformers.

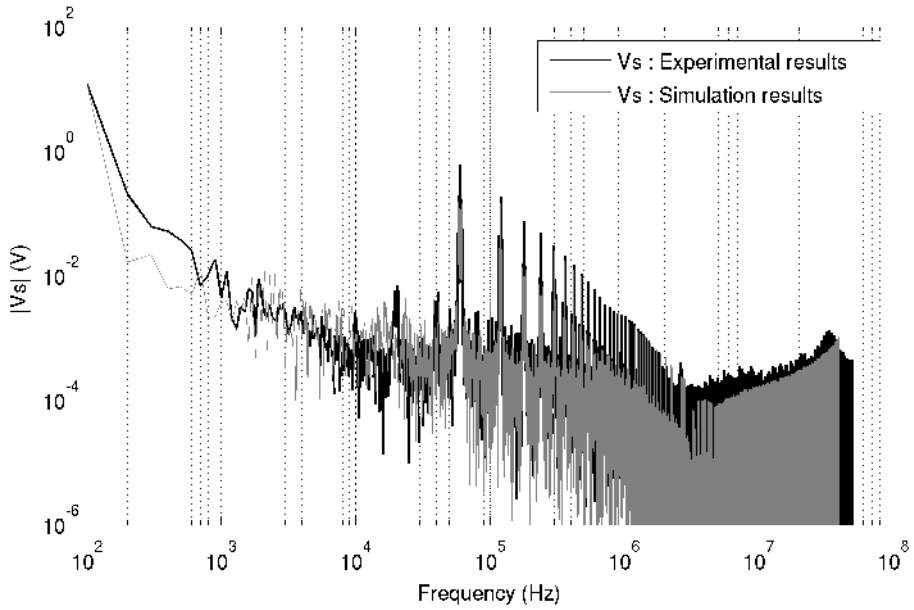

Fig. 10: Output voltage spectrum, simulation results versus experimental results.

III.2 Frequency spectrum of common mode current

In addition to the output voltage of the multicell inverter, the insertion impedance of the ICTs must be taken into account to calculate the common-mode currents. Theoretical expression of this relationship is given in equation 8. V_n are the voltages at the output of each switching cells and Y_{nm} admittances are derived from the Z matrix defined in equation 6 using relation 7.

$$[Y]=[Z]^{-1} \tag{7}$$

$$I_{CM}=\frac{\sum_{m=1}^{q}\sum_{n=1}^{q} Y_{nm}V_n}{1+\frac{Z_{CM}}{Z_L}+Z_{CM}\sum_{m,n=1}^{q} Y_{nm}} \tag{8}$$

Regarding equation 8, the source term, the insertion impedance and the global common mode impedance Z_{CM} defined at the output of the power converter can not be easily identified. However, assuming that the intercell transformers are quite identical, as defined in II.1, a simplified expression is given by equation 9.

$$I_{CM}=\frac{\frac{1}{q}\sum_{n=1}^{q} V_n}{Z_{CM}+2\frac{Z_{OC}-\sqrt{Z_{OC}\left(Z_{OC}-Z_{SC}\right)}}{q}\left(1+\frac{Z_{CM}}{Z_L}\right)} \tag{9}$$

The main disturbance source is given by the sum of the q output voltages of the switching cells. The contribution of the ICTs impedances Z_{CO} and Z_{SC} can be clearly identified, and the filtering effect on the common mode current is confirmed.

Figure 11, a final comparison between the common-mode current computed using the proposed model and the common-mode current measured on the prototype validates this approach. Despite the good correlation between these results, they must be treated with a critical eye. Indeed, this model is very dependent on measurement errors, as wiring measurement compensations, especially during impedance measurement of ICTs. These measurements must be carried out with great care.

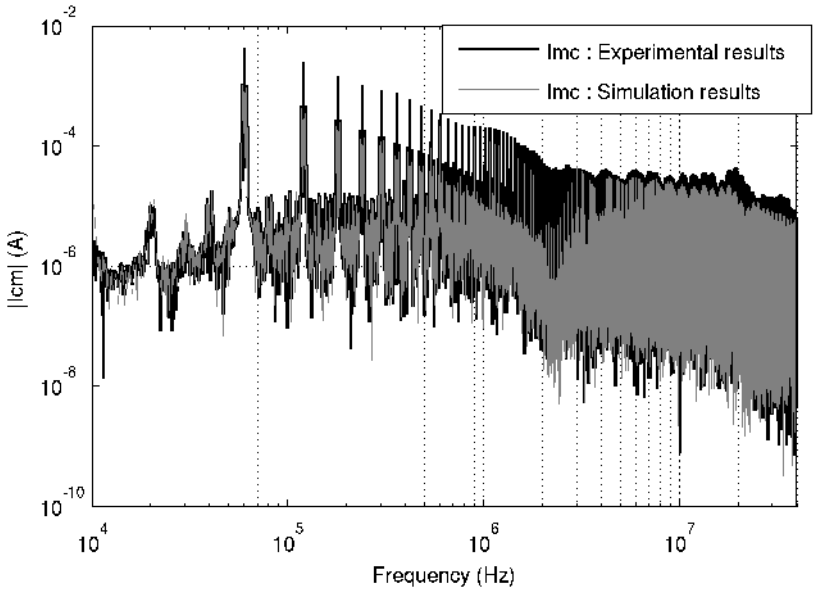

Fig. 11: Spectrum comparison between measured and simulated Common-mode currents

III.3 Positive effects on common-mode conducted interferences

The experimental data of the common mode voltage spectrum between a two-level inverter and a six level multicell inverter with TICs are compared figure 12. These measurements have been made with the same cable and the same load and for identical output RMS currents.

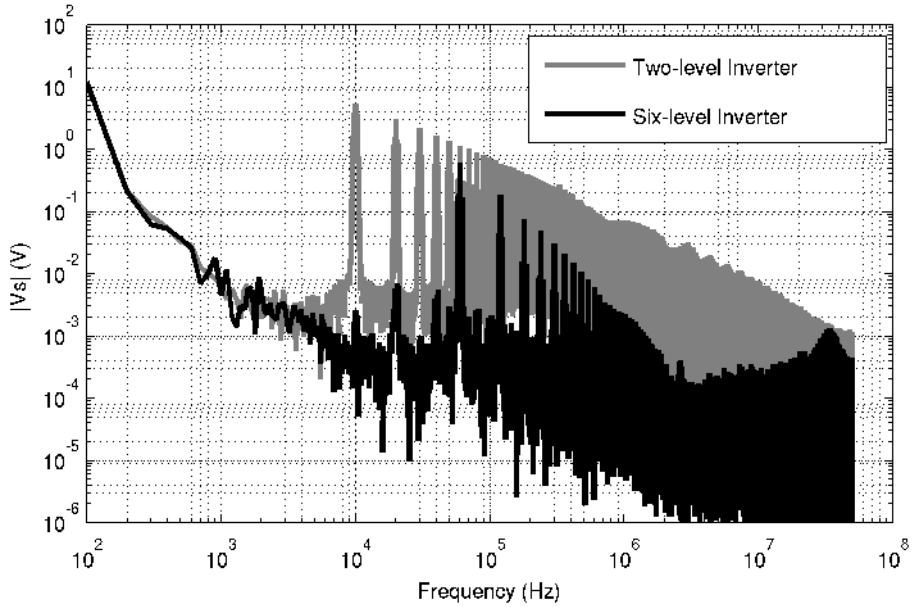

Fig. 12: Common-mode voltage spectrum (Experimental data)

As described previously, the results presented figure 12 show that the frequency of the first harmonic in the case of the multicell inverter is six time the switching frequency [9], and that the spectrum amplitude decreases rapidly until twenty megahertz compared to the two-level inverter. This is due to the natural filtering contribution of ICTs. Thus, the spectral content of the common mode voltage is significantly reduced, giving to the designer the opportunity to work on the PWM schemes in order to optimize the spectrum density. Such digital controls are currently studied in SATIE laboratory, they allow for example to reduce the amplitude of the fundamental (q x 10kHz) and harmonics but with a controlled increase in spectral density at lower frequencies. The modeling process is therefore very useful because these control schemes can be worked out using simulation tools.

Conclusion

An EMC oriented modeling process of a PWM Multicell Interleaved Inverter using Intercell Transformers has been proposed. In order to build this model, some experimental data have to be measured, as the load impedance or the switching cells voltage transients. However, the critical element concerning the model accuracy remain the intercell transformer. As a result, the simulated EMC relevant quantities are very closed to the measured ones, and the modeling process is validated. Although these new structures are complex, spectral density is greatly reduced compared to classical two-level inverter. Designers can use this extra freedom to define different control strategies that optimize the distribution of spectral content, and the electrical model of the power converter is therefore required to optimize these different control strategies.

References

[1] P.-L. Wong, P. Xu, B. Yang, and F. C. Lee, "Performance improvements of interleaving VRMs with coupling inductors," IEEE Trans. Power Electronics., vol. 16, no. 4, pp. 499–507, Jul. 2001.

[2] F. Forest, E. Labouré, T. A. Meynard, and V. Smet, "Design and Comparison of Inductors and Intercell Transformers for Filtering of PWM Inverter Output", IEEE Trans. Power Electronics., vol. 24, no. 3, pp. 812–820, Mar. 2009.

[3] E. Labouré, A. Cunière, T. Meynard, F. Forest, E.Sarraute, "A theorical approach to InterCell Transformer, application to interleaved converters", IEEE Trans. Power Electronics., vol. 23, n°1, pp. 464-474, Jan. 2008.

[4] O. Lucía; L.A. Barragán, J.M. Burdío, O. Jiménez, D. Navarro and I. Urriza, "A Versatile Power Electronics Test-Bench Architecture Applied to Domestic Induction Heating", IEEE transactions on Industrial Electronics, vol 58, march 2011.

[5] Labrousse, D. Revol, B. Costa, F. "Common-Mode Modeling of the Association of N-Switching Cells: Application to an Electric-Vehicle-Drive System", IEEE Trans. Power Electronics., vol. 25, n°11, pp. 2852-2859, Jun. 2010

[6] F. Costa, C. Vollaire, R. Meuret, "Modeling of conducted common mode perturbations in variable-speed drive systems", IEEE Transactions on EMC Vol. 47, Nov. 2005

[7] C. Gautier, B. Revol, F. Costa, J. Genoulaz, "Cable Modelling for Common Mode Interference Estimation in Embedded Power Electronic Systems", EMC Europe Workshop, Paris, France, June 14-15, 2007.

[8] G. Andrieu, L. Koné, F. Bocquet, B. Démoulin, and J-P. Parmantier, *" Multiconductor reduction technique for modeling common-mode currents on cable bundles at high frequency for automotive applications"*, IEEE Transactions on Electromagnetic Compatibility, Vol. 50, No. 1, February 2008

[9] J. Mon, D. Gonzalez, J. Gago, J. Balcells, R. Fernandez, I. Gil, "Contribution to conducted EMI reduction in multiconverter topology", Proc. IEEE IECON 2009, pp 12